J. Phys. C: Solid State Phys., Vol. 6, 1973. Printed in Great Britain.

Low temperature Hall measurements on the X_{1c} electrons in GaAs

M K R Vyas†, G D Pitt† and R A Hoult‡

† Standard Telecommunication Laboratories Ltd, London Road, Harlow, Essex

‡ Clarendon Laboratory, Oxford University

MS received 5 October 1972

Abstract. Hall measurements to 120 K at 50 kbar have been carried out for electrons in the ⟨100⟩, X_{1c}, satellite valleys in epitaxial and bulk grown GaAs for carrier concentrations in the range 10^{14}–10^{18} cm^{-3}. Two distinct impurity levels have been found to be associated with the X_{1c} minima; estimates of activation energies 0·145 ± 0·02 eV and 0·066 ± 0·01 eV have been obtained for carrier concentrations near 10^{15} cm^{-3}. The activation energies of these levels decreased with increasing carrier concentration. Theoretical analysis of mobility–temperature curves has shown intervalley scattering to be dominant for purer samples while for the heavily doped bulk grown samples space-charge scattering becomes more important. A best estimate of the (X_{1c}–X_{1c}) deformation potential field, D_{XX}, of 0·8 × 10^9 eV cm^{-1} for a deformation potential E_1 of 5·0 eV has been obtained. A single-valley density of states effective mass $m^* = 0{\cdot}41m$ was required to fit the experimental data. The results are relevant to the high electric field calculations used to assess the performance of transferred electron devices. The absolute mobilities at 300 K were estimated as (*a*) intervalley 500 cm^2 V^{-1} s^{-1}, (*b*) polar optical 1100 cm^2 V^{-1} s^{-1}, (*c*) deformation potential 2900 cm^2 V^{-1} s^{-1}. An empirical relation between the effective space charge cross section (N_sA) and carrier concentration (n) is found to follow a $N_sA \propto n^{1/3}$ power law.

1. Introduction

The electrical properties of electrons in the higher lying subsidiary conduction band minima of semiconductors such as GaAs and InP are of interest since they are involved in the mechanism which gives rise to transferred electron devices. Under high electric fields (3 kV cm^{-1}) electrons in GaAs transfer from a high mobility, low effective mass Γ_{1c} state to low mobility minima in the ⟨100⟩ direction (X_{1c}). A negative differential conductivity results, and microwave oscillations can be produced in a suitable circuit. The scattering strengths between the different minima and their band parameters are important for a full understanding of the device possibilities. Using the parameters obtained in conjunction with similar results for different III–V compounds, we can then postulate the exact conduction band structure for a particular transferred electron device application and the appropriate alloy system to realize it.

We describe here Hall measurements to low temperatures on n type GaAs for carrier concentrations in the range 10^{14}–10^{18} cm^{-3}, after the electrons have been transferred to the X_{1c} minima by the application of very high pressures. This is the first time that rigorous single crystal transport measurements have been carried out under such condi-

tions. The results provide mobility/temperature variations which have been analysed in terms of all possibly likely scattering mechanisms to 120 K. The simple theoretical fits to the data have allowed us to estimate the X_{1c} effective mass, and particularly the deformation potential field for X_{1c}–X_{1c} intervalley scattering once the band deformation potential is known. The relative importance of the different scattering mechanisms are discussed and compared with results obtained in other materials, for example, GaP where electrons occupy $\langle 100 \rangle$ minima. Previously the importance of the different scattering mechanisms in GaAs had been estimated by fitting to the low field mobility determined by Pitt and Lees (1970). Fawcett *et al* (1969) estimated that both intervalley and polar optical scattering were of equal importance, after using the deformation potential field of 1×10^9 eV cm^{-1} for intervalley scattering in the $\langle 100 \rangle$ valleys in Si (Long 1960).

High pressure Hall measurements have indicated that impurity levels associated with the higher lying minima, and degenerate with levels in the lowest conduction band, can exist. Many such levels have now been observed in a number of III–V and II–VI compounds. In GaAs two levels near 0·14 and 0·07 eV below the X_{1c} minima were found by Pitt and Lees (1970), but these measurements were carried out at room temperature and the errors were large. The low temperature Hall measurements should allow us to confirm the existence of these levels.

2. Experimental

The very high pressure single crystal apparatus has been described in detail by Pitt (1968). This was modified for low temperature measurements by enclosing the Bridgman anvils in insulated coils through which liquid N_2 was pumped using N_2 gas (figure 1). The single crystals were cut into 2 mm diameter cloverleafs, ohmic tin contacts were soldered to the lobes, and the crystal was placed at the centroid of an MgO loaded epoxy Bridgman ring and potted in epoxy. The leads and the chromel alumel thermocouple were passed out through grooves in the gasket. Good temperature regulation to within 2 K could be obtained.

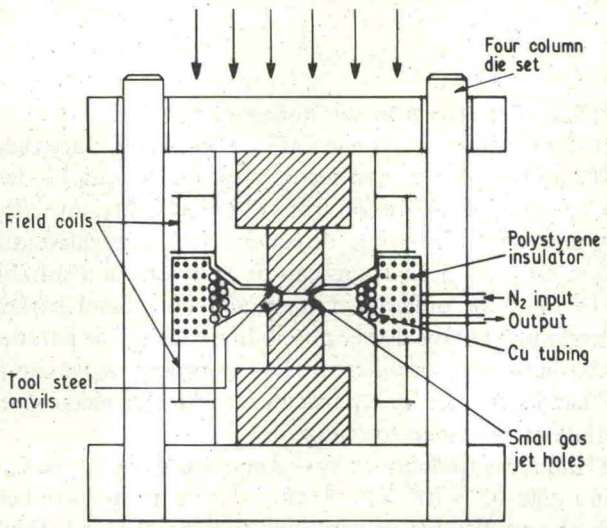

Figure 1. Cross section of opposed anvil high pressure apparatus including the low temperature modification.

The equipment is nonhydrostatic below 25 kbar, but above this pressure it closely approximates to hydrostatic conditions. This was shown by piezoresistance measurements on n type Si, where the electrons occupy off-centre ⟨100⟩ minima whose degeneracy can be lifted by nonhydrostatic stress. Measurements on other materials have also confirmed this analysis of the stress system. At low temperatures however it is likely that the stress system alters, and so only ⟨111⟩ orientation GaAs crystals were studied. From the symmetry of the apparatus and the stress system the degeneracy of electrons in the ⟨100⟩ valleys would not be removed at low temperatures. Similar measurements on n type Ge have confirmed that this is the case (Pitt, unpublished).

Experimental runs were made by increasing the pressure to 50 kbar and reading Hall measurements during electron transfer to X_{1c} minima using a Keithley 150B microvoltmeter. The temperature was then lowered slowly at the rate of about 2 K min^{-1} to 120 K, and thereafter readings were taken on the heating cycle. At all times the load was kept constant. Up to four runs on a crystal from each slice were made.

3. Crystals

The crystals were prepared at STL using bulk gradient freeze techniques, and for the purer samples liquid epitaxial techniques were used. In the latter cases the ⟨111⟩ crystals were grown at the same time as ⟨100⟩ specimens by Dr P D Greene, and the results in table 1 compare the data at 300 K and 77 K. We found, in common with other workers, that the mobilities of the ⟨100⟩ orientated samples were greater than for the ⟨111⟩ crystals; also there was a definite increase in carrier concentration for the ⟨111⟩ slices. No significant difference in mobility or carrier concentration could be detected for deposition on A (Ga) or B (As) faces. A considerable amount of speculation has been offered to explain this effect, and the correct solution is probably a combination of a number of mechanisms; for instance the growth rates can differ depending on the growing face resulting in different amounts of impurity incorporation; we note however that no significant difference in epitaxial thickness was found for the ⟨100⟩ and ⟨111⟩ epitaxial layers. We do not discuss this problem further except to note that the compensation in the ⟨111⟩ slices was more pronounced. The dopants were Se for the bulk samples and Sn for the epitaxial samples.

4. High pressure measurements

4.1. Room temperature

The results on all samples to 50 kbar at room temperature are summarized in table 2. The results show different amounts of carrier loss to deep impurity levels below the X_{1c} minima, that is R_H/R_{H0} does not return to unity by 50 kbar. These emerge into the forbidden gap on the application of pressure. At atmospheric pressure they are higher than the bottom of the Γ_{1c} minimum. These results allow us, however, to calculate the impurity activation energies (see the following section on analysis) which are given in the table. The ratio of R_H/R_{H0} at 50 kbar gives a quick estimate of the carrier loss after the transfer process has been completed. We took the condition for zero trap out to be that $R_{H(50)}/R_{H0}$ should be 0·90 (Pitt and Lees 1970) after making reasonable assumptions about the ellipsoidal nature of the ⟨100⟩ minima. It was further found that the X_{1c}

Table 1. Hall data for ⟨100⟩ and ⟨111⟩ slices at 300 K and 77 K

GaAs sample number	⟨100⟩ slice n_{300K} (cm^{-3})	n_{77K} (cm^{-3})	μ_{300K} ($cm^2 V^{-1} s^{-1}$)	μ_{77K} ($cm^2 V^{-1} s^{-1}$)	ρ_{300K} (Ω cm)	ρ_{77K} (Ω cm)	⟨111⟩ slice n_{300K} (cm^{-3})	n_{77K} (cm^{-3})	μH_{300K} ($cm^2 V^{-1} s^{-1}$)	μH_{77K} ($cm^2 V^{-1} s^{-1}$)	ρ_{300K} (Ω cm)	ρ_{77K} (Ω cm)
Epitaxial 7LE103	2.4×10^{13}	2.35×10^{13}	8200	94000	38.11	2.833	4.5×10^{14}	3.74×10^{14}	6420	57000	2.17	0.294
Epitaxial 4LE149	2.1×10^{15}	1.75×10^{15}	7700	107880	0.38	0.033	4.4×10^{15}	3.58×10^{15}	6550	25574	0.22	6.83×10^{-2}
Epitaxial 3LE132	3.9×10^{14}	3.81×10^{14}	7600	404832	2.22	0.041	1.4×10^{15}	2.03×10^{14}	6800	27486	0.66	1.121
Bulk 244F	1.05×10^{17}	9.14×10^{16}	3600	3065	1.68×10^{-2}	2.2×10^{-2}	1.05×10^{17}	9.14×10^{16}	3600	3065	1.68×10^{-2}	2.2×10^{-2}
Bulk 548	7.15×10^{17}	8.56×10^{17}	3430	3243	2.5×10^{-3}	1.12×10^{-3}	7.15×10^{17}	8.56×10^{17}	3430	3248	2.5×10^{-3}	1.12×10^{-3}

Table 2. Summary of high pressure results at 300 K

GaAs crystal	Hall mobility at 50 kbar ($cm^2 V^{-1} s^{-1}$)	$\frac{\mu_H\langle 000\rangle}{\mu_H\langle 100\rangle}$	$N_D - N_A$ cm^{-3} at 50 kbar	$\frac{R_{H(50)}}{R_{HO}}$	$\frac{\rho}{\rho_0}$	Impurity level activation energy (eV)
Epitaxial 7LE103	260	25.68	3.38×10^{14}	1.33	29.0	0.145
Epitaxial 4LE149	225	30.47	3.3×10^{15}	1.33	30.0	0.102
Epitaxial 3LE132	290	23.45	1.48×10^{15}	1.00	25.0	0.100
Bulk 244F	155	23.23	3.63×10^{16}	2.89	65.0	0.105
Bulk 548	142	24.15	4.95×10^{17}	1.44	32.0	0.051

mobilities for our ⟨111⟩ samples were lower than a typical result by Pitt and Lees (1970) for ⟨100⟩ material, for example, for $n \sim 10^{15}$ we obtain here a value of $290 \pm 30\ \mathrm{cm^2\ V^{-1}\ s^{-1}}$, which compares with a ⟨100⟩ crystal value of $350 \pm 30\ \mathrm{cm^2\ V^{-1}\ s^{-1}}$.

Typical high pressure variations of normalized resistivity (ρ/ρ_0), Hall constant (R_H/R_{H0}) and Hall mobility (μ_H/μ_{H0}) are shown in figure 2 for 7LE103. The band transfer

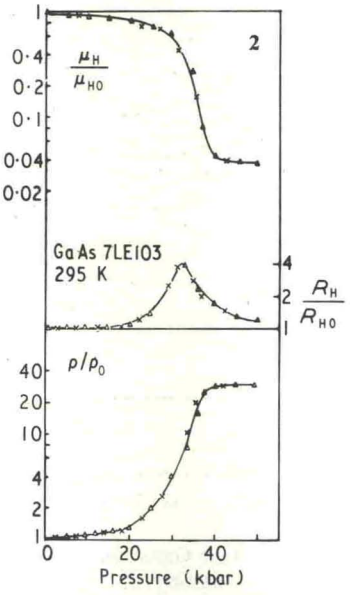

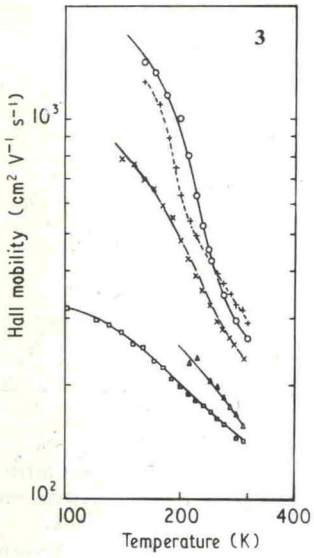

Figure 2. Normalized resistivity (ρ/ρ_0), Hall constant (R_H/R_{H0}), and Hall mobility (μ_H/μ_{H0}) plots for GaAs 7LE103 to 50 kbar.

Figure 3. Hall mobility against temperature plots to 100 K for n type GaAs single crystals at 50 kbar. The electrons occupy the X_{1c} minima. ○7LE103; × 4LE149; + 3LE132; △ bulk 244F; □ bulk 548.

effect where the mobility drops as the electrons occupy the heavy mass X_{1c} minima is well illustrated. The maximum in R_H/R_{H0} is a consequence of the two-carrier situation where the mobilities are very different.

4.2. Low temperature

The Hall mobilities to 120 K are shown in figure 3. For samples with lower carrier concentrations the mobility variation is more marked, while the more heavily doped samples show a shallower mobility increase to low temperatures. Near 300 K the $\mu \propto T^s$ relation varied from $s = 2{\cdot}6$ for purer material ($n \sim 10^{14}\ \mathrm{cm^{-3}}$) to 1·4 for $n \sim 10^{17}\ \mathrm{cm^{-3}}$.

The carrier concentrations of these samples was calculated from the relation

$$n = r(R_H e)^{-1}$$

where r (the scattering constant) was taken as unity. Pitt and Lees (1970) estimated this to be ~1·04 for the X_{1c} minima following reasonable assumptions about the ellipsoidal nature of the minima. The carrier concentrations are plotted in figure 4. We can see that samples 548 and 3LE132 are not trapping out until lower temperatures implying that the

activation energies for these samples are lower, provided the compensations are similar. The resistivity variations are plotted in figure 5.

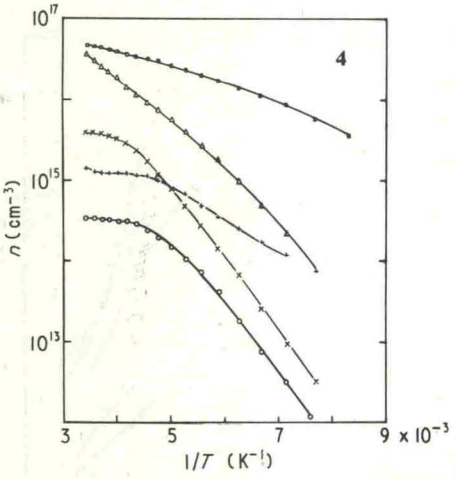

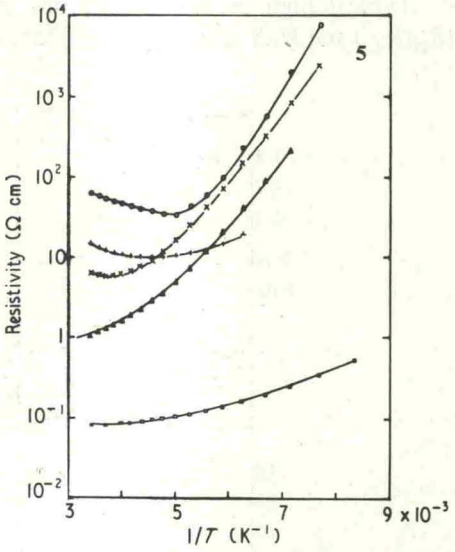

Figure 4. Carrier concentration plots to 100 K for n type GaAs single crystals at 50 kbar. The electrons occupy the X_{1c} minima. ○7LE103; × 4LE149; + 3LE132; △244F (bulk); □548 (bulk).

Figure 5. Resistivity variations to 100 K for n type GaAs single crystals at 50 kbar. The electrons occupy the X_{1c} minima. ○7LE103; × 4LE149; △244F; + 3LE132; □548.

5. Analysis

5.1. Room temperature data

The analysis of the room temperature data has already been described in detail by Pitt and Lees (1970), and the same procedure was adopted here. Basically we analyse the results by fitting the charge balance equation:

$$N_D - N_A = n_\Gamma + n_X + n_d \tag{1}$$

where N_D and N_A are the total number of donors and acceptors respectively, n_Γ and n_X are the number of electrons in the Γ_{1c} and X_{1c} minima, while n_d is the number of electrons on donor sites. $N_D - N_A$ at atmospheric pressure was taken to be the measured carrier concentration, since all the electrons will be ionized to the Γ_{1c} minimum. n_d can be calculated from a simple expression involving N_D and the X_{1c} donor impurity activation energy. N_D was calculated using the measured mobility value and the empirical Brooks–Herring relation used by Wolfe *et al* (1969) for 77 K data. For carrier concentrations above 10^{18} cm^{-3} this is not really valid, since the scattering becomes more complex in the Γ_{1c} minimum and multiple scattering events will occur, that is the Born approximation is not valid. We have extrapolated the Brooks–Herring data for sample 548, however, and estimate that little error will be incurred.

The theoretical fit to the mobility data was not much different from our previous results where the sub-band energy $E(X_{1c} - \Gamma_{1c})$ at atmospheric pressure was taken as

0·38 ± 0·02 eV and the X_{1c} density of states effective mass in one minimum was 0·41m. The activation energies are given in table 2 and will be discussed in §6 when they are compared with the low temperature results.

5.2. *Low temperature data*

5.2.1. Mobility. We analyse first the mobility variations with temperature. Our approach has been extremely simple assuming spherical X_{1c} minima. Fletcher and Butcher (1973) have derived a method for analysing polar optical (PO) scattering in ellipsoidal minima and their interpretation of the results on the purer samples will probably be more rigorous. Rather than develop a technique for the analysis of the data as they have done however, we have used the results to try and obtain estimates of the different scattering parameters, which are useful in high electric field calculations. This is particularly the case for the deformation potentials which involve the X_{1c} minima. It will be shown below that the values used by Fletcher and Butcher (1973) fall within the limits of error determined by us. We have analysed the results using the usual reciprocal addition of mobilities, although it is appreciated that it is difficult to define a polar optical scattering relaxation time at low temperatures.

$$\frac{1}{\mu} = \sum_i \frac{1}{\mu_i} \tag{2}$$

where μ_i represents the different scattering mechanisms considered, that is, equivalent intervalley (IV) μ_{IV}, ionized impurity (I) μ_I, space charge (SC) μ_{SC}, and deformation potential scattering (DP) μ_{DP}, polar optical (PO) μ_{PO}.

We have reduced the different mobility equations to the following forms (CGS units).

$$\mu_{PO} = 19{\cdot}43\, T^{1/2} \left\{ \exp\left(\frac{400}{T}\right) - 1 \right\} \exp(-\xi)\, G \tag{3}$$

$$\mu_{DP} = \frac{3{\cdot}87 \times 10^8}{E_1^2 T^{3/2}} \tag{4}$$

$$\mu_{SC} = \frac{5{\cdot}1295 \times 10^9}{N_S A T^{1/2}} \tag{5}$$

$$\mu_I = \frac{3{\cdot}28 \times 10^{15} (m/m^*)^{1/2} \epsilon_0^2 T^{3/2}}{(2N_A + n)\{\ln(b+1) - b/(b+1)\}} \tag{6}$$

where

$$b = \frac{1{\cdot}29 \times 10^{14} (m^*/m)\, \epsilon_0 T^2}{n^*} \tag{7}$$

$$n^* = n + \left(\frac{(n + N_A)(N_D - N_A - n)}{N_D} \right).$$

The equation for PO scattering is the simple equation originally used by Ehrenreich (1959), and the function $\exp(-\xi)\, G$ is plotted in that paper. The dielectric constants ϵ_∞ and ϵ_0 have been taken as 10·82 and 12·53 at 300 K respectively (Hilsum 1965); the angular frequency of the LO phonon at the X point was taken as $4{\cdot}90 \times 10^{13}$ rad s^{-1} at 50 kbar after taking the value at atmospheric pressure of Waugh and Dolling (1963),

and assuming that the 0·16% increase/kbar found at $\boldsymbol{k} = 0$ by Buchenauer *et al* (1971) still holds at the zone edge; the reduced atomic mass M is $6{\cdot}02 \times 10^{-23}$ g.

The equation for DP scattering is standard; the density at 50 kbar is 5·60 g cm^{-3}, after correcting for the volume change using the data of McSkimin *et al* (1967). These data were also used to calculate the lattice constant at 50 kbar, that is 5·537 Å. E_1 is the effective deformation potential of the conduction band.

Space charge scattering has been discussed by Weisberg (1961); N_S is the concentration of space charge regions, and A is the effective scattering area.

For ionized impurity scattering we have used the Brooks–Herring equation. For IV scattering we used Herring's (1955) original equation where the LO phonons have a characteristic temperature of $T_i = 400$ K at 50 kbar. For minima situated in from the zone edge the analysis becomes more complicated since more than one phonon is involved. This type of analysis was used on the n type Si mobility data to low temperatures by Long (1960) who found that intervalley scattering dominated at room temperature. He used his results to determine a value of the coupling constant D_{XX} for intervalley scattering (nowadays the terminology is to call this parameter the intervalley deformation potential or deformation potential field). This is proportional to the square root of ω_l/ω_A, and is a measure of the strength of coupling of the LO phonons involved in intervalley scattering to the acoustic phonons involved in DP scattering. This formalism was reduced by Conwell (1966) to the form:

$$\alpha = \omega_l/\omega_A = \frac{2D_{XX}^2 u_i^2}{E_1^2 \omega_l^2} \tag{8}$$

where u_i is the longitudinal sound velocity taken as $4{\cdot}73 \times 10^5$ cm s^{-1} (McSkimin *et al* 1967).

The analysis of the mobility/temperature results treats E_1 and D_{XX} (ie α) as variable parameters for the purer samples. For the less pure samples space charge scattering was required, and here the variable parameters resolve to N_S and A (eg equation 5). To begin we can take initial values of E_1 by comparison with other III–V and II–VI compounds. We find that the most acceptable values lie in the region of 7 eV for all the III–V compounds (eg Rode 1970), but this is for the Γ_{1c} minimum and more recent values for InSb are nearer 14 eV (Zawadzki and Szymanska 1972). For data on $\langle 100 \rangle$ minima we compare with GaP. Toyama *et al* (1969) could fit their data with values between $8 \leqslant E_1 \leqslant 12$ eV while Epstein (1966) used a value of 12·7 eV. We may calculate the deformation potential from the observed shift of the $\langle 100 \rangle$ minima with pressure, where

$$\frac{dE_g}{dP} = E_1 3(S_{11} + 2S_{12}) \tag{9}$$

where S_{ij} are the components of the compliance tensor and

$$E_1 = \Xi_d + \tfrac{1}{3}\Xi_\mu - a \tag{10}$$

where Ξ_d is the dilational deformation potential, and Ξ_μ is the shear deformation potential; a is the deformation potential constant of the valence band. Thus we could calculate E_1 provided we have measured the compliance coefficients, but typical values for these where dE_g/dP (100) is taken as $\sim 1{\cdot}5 \times 10^{-6}$ eV bar^{-1} give deformation potentials near 1 eV for the $\langle 100 \rangle$ states in GaAs and GaP, which is low. Alternatively a calculation based on equation (10) is even less reliable since experimental values of a, for example in Si, can vary from -7 to $+21$ (Costato and Reggiani 1970). For the $\langle 100 \rangle$ valleys in Si

using the low temperature mobility data of Long (1960) a value of 7·4 eV was obtained by Fawcett and Paige (1971) while for the ⟨100⟩ valleys in Ge they used a value of 5·99 eV. Conwell and Vassell (1968) used a deformation potential of 8·48 eV to fit the GaAs high field data. In the face of these discrepancies we decided to calculate fits to the mobility data beginning with a deformation potential of 7 eV. Our remaining adjustable parameter was then D_{XX} for the undoped material, and fits to the mobility are shown in figures 6 and 7. A combination of DP, PO and IV scattering fitted the data within experimental error, although the experimental points for 7LE103, figure 6, were slightly higher than the theoretical curve for $T < 200$ K. These fits were obtained by taking the value of D_{XX} as $1{\cdot}2 \times 10^9$ eV cm^{-1}. On this basis also, it was found that for sample 4LE149, figure 8, we were forced to include space charge scattering, with a value of $N_S A$ of $2{\cdot}5 \times 10^5$ cm^{-1}. These results show that at room temperature the dominant scattering mechanism is intervalley scattering, whereas the results of Fawcett *et al* (1970) indicated that both PO and IV scattering made approximately equal contributions. It should be noted however

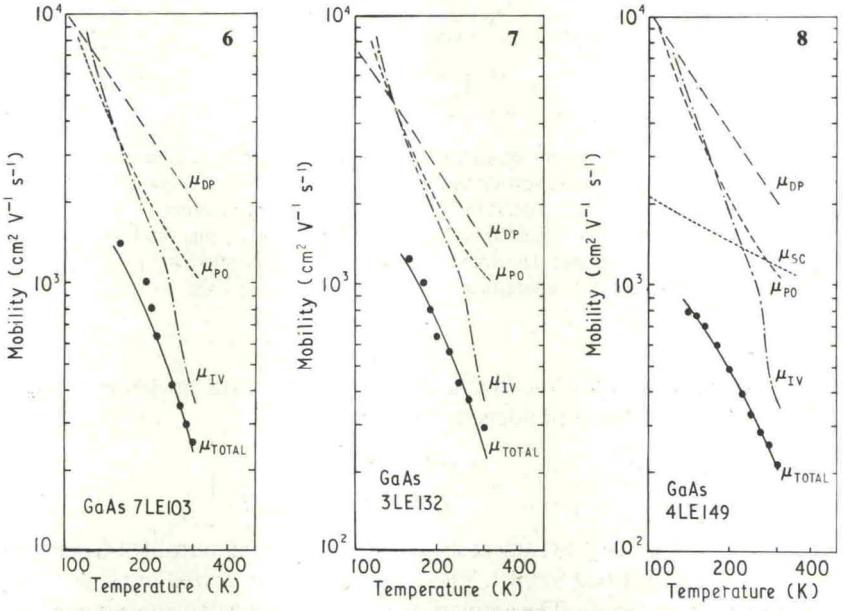

Figure 6. Calculated mobilities for different scattering mechanisms for crystal 7LE103 at 50 kbar. Intervalley scattering is dominant at 300 K.

Figure 7. Calculated mobilities for different scattering mechanisms for crystal 3LE132 at 50 kbar. Intervalley scattering is dominant at 300 K.

Figure 8. Calculated mobilities for different scattering mechanisms for crystal 4LE149 at 50 kbar. Intervalley scattering is dominant at 300 K, but space charge scattering is required to give satisfactory agreement with experiment.

that they used an effective mass of 0·35m to obtain this result. If a mass of 0·41m had been used they would have predicted a similar result to us, and found that intervalley scattering was more important. For the higher concentration materials (figures 9 and 10) we find that considerable space charge scattering is present, and we have to fit the data using a combination of I, PO, IV, and SC.

Throughout the calculations we have ignored the effect of piezoelectric scattering because the effect is minimal over the whole temperature range.

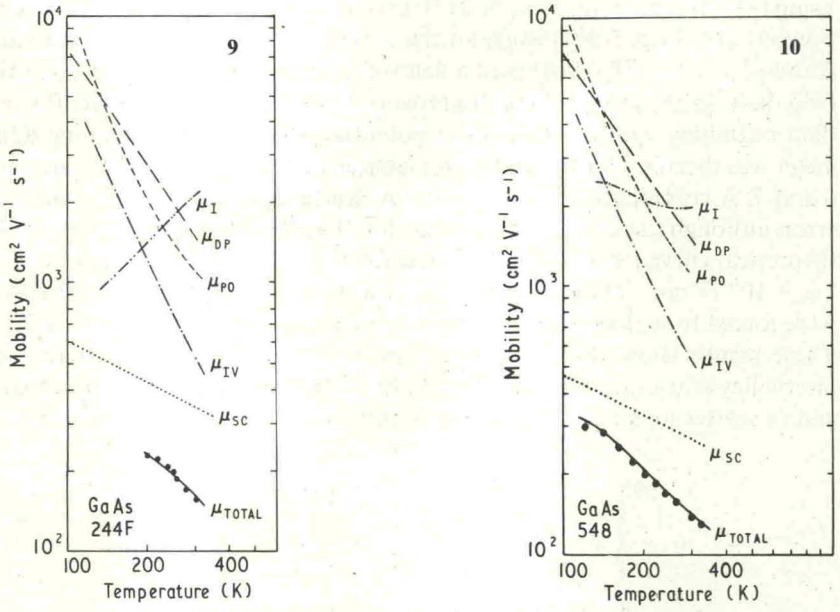

Figure 9. Calculated mobilities for different scattering mechanisms for crystal 244F at 50 kbar. The dominant scattering mechanism at 300 K is space charge scattering. Ionized impurity scattering is required to fit the data at lower temperatures.

Figure 10. Calculated mobilities for different scattering mechanisms for bulk grown crystal 548 at 50 kbar. The dominant scattering mechanism at 300 K is space charge (SC) scattering, and at low temperatures ionized impurity (I) scattering is required.

5.2.2. Carrier concentration. We have analysed the data presented in figure 4 using the single valley model and nondegenerate statistics:

$$\frac{n(n+N_A)}{N_D-N_A-n}=\frac{2(2m^*kT)^{3/2}}{gh^3}\exp\left(\frac{-E_d}{kT}\right) \tag{11}$$

where g is the spin degeneracy of 2, N_D and N_A were determined from the data of Wolfe *et al* (1970) as described in § 4.1. These data are summarized in table 3 together with the deduced donor energies. The activation energies are plotted against carrier concentration in figure 11, and compared with the data determined at room temperature (table 2) and the previous results of Pitt and Lees (1970). We find that two distinct impurity levels exist with activation energies (for $n \sim 10^{15}$ cm^{-3}) of 0·07 and 0·14 eV. Both activation energies decrease for higher carrier concentrations, for example, for $n \sim 10^{18}$ cm^{-3} we obtain energies near 0·04 and 0·10 eV. The smaller activation energy may be reconciled to the simple hydrogenic model, and is comparable with similar donor energies for GaP (eg Montgomery 1968). The higher donor energy agrees with Pitt and Lees (1970). The energies obtained by Adler (1969) were between 0·14–0·21 eV, on sulphur doped material from resistivity measurements at room temperature. These latter measurements also gave an energy of 0·30 ± 0·02 eV on some unintentionally doped bulk material. Extensive measurements on sulphur doped $GaAs_{1-x}P_x$ alloys by Craford *et al* (1968) again revealed two levels relative to the X_{1c} minima of 0·16 and 0·06 eV which is in general agreement with our result. The carrier concentrations were typically 5×10^{17}–10^{18} cm^{-3} however, and the energies are higher than ours. We may explain this simply by noting

Table 3. Calculated values of N_D, N_A and E_D from temperature data

Sample	N_D cm^{-3}	N_A cm^{-3}	E_D (eV)
7LE103	$1{\cdot}26 \times 10^{15}$	8×10^{14}	$(0{\cdot}142 \pm 0{\cdot}01)$
4LE149	$7{\cdot}18 \times 10^{15}$	$2{\cdot}78 \times 10^{15}$	$(0{\cdot}118 \pm 0{\cdot}01)$
3LE132	$3{\cdot}51 \times 10^{15}$	$2{\cdot}11 \times 10^{15}$	$(0{\cdot}104 \pm 0{\cdot}01)$
Bulk 244F	$2{\cdot}62 \times 10^{17}$	$1{\cdot}57 \times 10^{17}$	$(0{\cdot}091 \pm 0{\cdot}01)$
Bulk 548	$7{\cdot}58 \times 10^{17}$	$0{\cdot}43 \times 10^{17}$	$(0{\cdot}036 \pm 0{\cdot}01)$

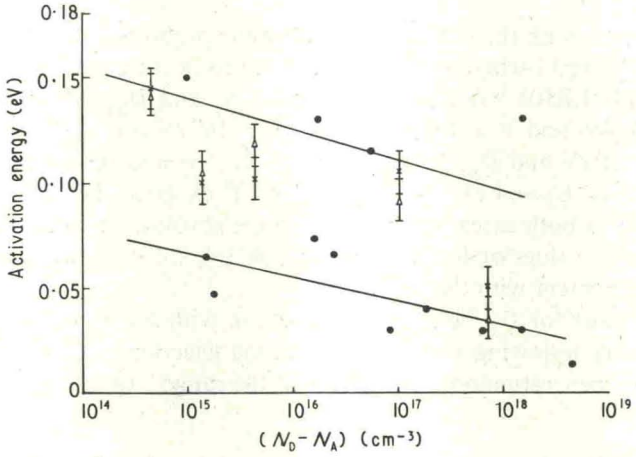

Figure 11. Calculated donor activation energies relative to the X_{1c} minima at 50 kbar. × Room temperature data: △ low temperature data; ● Pitt and Lees (1970).

that S donors in GaP and GaAs have higher activation energies than Se, Si, Sn, and Te. Our samples were Se and Sn doped, so the preliminary inference is that our results indicate two Se or Sn levels relative to the ⟨100⟩ minima.

6. Discussion

The analysis of the mobility data to low temperatures in § 5.2 revealed that for a deformation potential of 6 ± 1 eV we require a deformation potential field for intervalley scattering D_{XX} of $1{\cdot}0 \pm 0{\cdot}2 \times 10^9$ eV cm^{-1}. This latter parameter is particularly important for the calculation of high electric field transport properties, and the assessment of a material for device purposes. An experimental result of this type is also useful to compare with theoretical calculations on the different intervalley scattering strengths. Our value is linked however with the initial value of E_1 that we take. To investigate this relationship further, we have taken different values of E_1 in the range 4 to 12 eV and tried again to fit the data. The data used to fit the mobility data given in figures 6–10 are summarized in table 4.

We find that as the E_1 drops then we require D_{XX} to decrease also, but find that acceptable agreement with experiment is confined to a remarkably small range of values, that is, $5 \leqslant E_1 \leqslant 7$ eV and $8 \times 10^8 \leqslant D_{XX} \leqslant 1{\cdot}2 \times 10^9$ eV cm^{-1}. For values outside

Table 4. Deformation potential data for ⟨100⟩ valleys in n type GaAs used in the mobility plots

Sample	Deformation potential, E_1 (eV)	Deformation potential field D_{XX} (eV cm^{-1})	$\frac{\omega_i}{\omega_A}$
7LE103	6·0	$1·0 \times 10^9$	4·36
3LE132	7·0	$1·2 \times 10^9$	3·2
4LE149	6·0	$1·0 \times 10^9$	4·36
Bulk 244F	7·0	$1·0 \times 10^9$	2·74
Bulk 548	7·0	$1·0 \times 10^9$	2·74

these limits, agreement with the μ/T slope and absolute mobility values are poor. This is well illustrated in figure 12 where we have attempted to fit the experimentally observed mobility for crystal 7LE103 using paired values of E_1 and D_{XX} which lie outside the range $5 \leqslant E_1 \leqslant 7$ eV and $8 \times 10^8 \leqslant D_{XX} \leqslant 1·2 \times 10^9$ eV cm^{-1}. The theoretical fit obtained for $E_1 = 10$ eV and $D_{XX} = 1·4 \times 10^9$ eV cm^{-1} is well below the experimental curve whilst the fit for $E_1 = 4$ eV and $D_{XX} = 7 \times 10^8$ eV cm^{-1} lies well above the experimental points. For both cases, agreement with the absolute mobility values and μ/T slope is bad. Coupled values of, for example, $D_{XX} = 1·4 \times 10^9$ eV cm^{-1} and $E_1 = 4$ eV give even worse agreement with the μ/T slope.

Our range of values for D_{XX} is in good agreement with the Si value determined by Long (1960). Recently, following a reassessment of the selection rules for scattering in Si by Streitwolf (1970), new estimates of this value in the range 3 to 5×10^8 eV cm^{-1} have

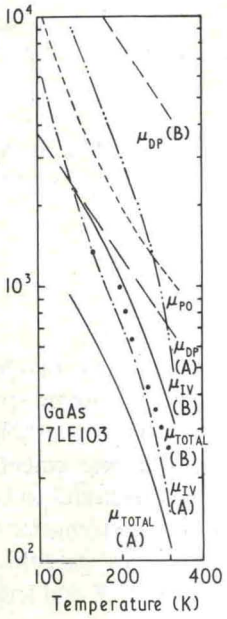

Figure 12. Calculated mobilities for different scattering mechanisms for crystal 7LE103 at 50 kbar. μ_{TOTAL} (A) refers to the total theoretical mobility fit for $E_1 = 10$ eV and $D_{XX} = 1·4 \times 10^9$ eV cm^{-1}. μ_{TOTAL} (B) refers to the fit for $E_1 = 4$ eV, and $D_{XX} = 7 \times 10^8$ eV cm^{-1}. These plots illustrate that values of E_1 and D_{XX} outside the range $5 \leqslant E_1 \leqslant 7$ eV and $8 \times 10^8 \leqslant D_{XX} \leqslant 1·2 \times 10^9$ eV cm^{-1} give poor fits. ● Experimental points.

been made by Jorgensen *et al* (1972) and Herbert *et al* (1972). James and Moll (1969) obtained $D_{XX} = 1{\cdot}3 \pm 0{\cdot}2 \times 10^9$ eV cm^{-1} for GaAs, but the X_{1c} mobility that they obtained using this value is much too low when compared with experimental total mobility of 320 cm^2 V^{-1} s^{-1} found by Pitt and Lees (1970). The mobility at 300 K requires that D_{XX} must be less than $1{\cdot}3 \times 10^9$ eV cm^{-1}. Rode (1972) has recently used a value of $D_{XX} = 1{\cdot}2 \times 10^9$ eV cm^{-1} to fit GaP mobility data.

In figure 13 we have plotted the values of $N_S A$ against carrier concentration (n) used by us to fit the mobility data with space charge scattering. The data are compared with values used by Toyama *et al* (1969) to fit the low temperature GaP data. It is accepted that

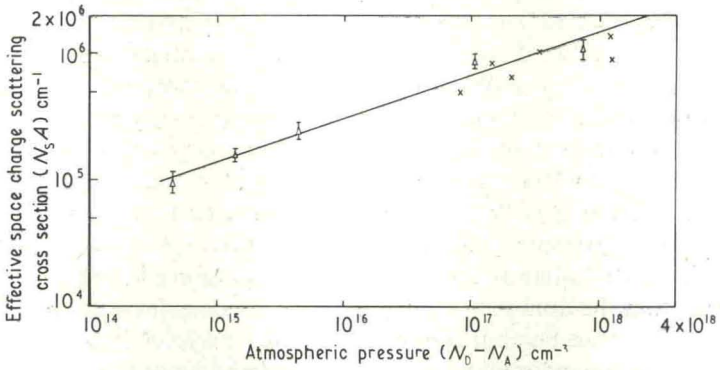

Figure 13. Plot of effective space charge scattering cross section $N_S A$ against atmospheric pressure ($N_D - N_A$). Results are compared with the results of Toyama *et al* (1969) for GaP. A power law of $N_S A \propto n^s$ where $s = 0{\cdot}33 \pm 0{\cdot}02$ is found. Similar plots of $N_S A$ against N_D and $N_D + N_A$ also give slopes within the experimental error. A plot of ($N_S A$) against N_A could not be fitted by a straight line without incurring large errors. At the lower electron concentrations values for $N_S A$ were found for crystals 3LE132 and 7LE103 by assuming that SC scattering was present, although the mobility data could be adequately fitted without this. △ Present results for GaAs; × Toyama *et al* (1969) for GaP.

SC scattering can only be used in the final analysis as an adjustable scattering mechanism which conveniently fits the data. The equation (5) used can only be an approximate relation since the shape of the space charge region could differ considerably from that of a sphere which we have used. The values of $N_S A$ and n for both GaAs and GaP on a log–log plot however do fall on a straight line with surprisingly little error, even allowing for a small discrepancy in effective masses for the two materials. The power law obtained is $N_S A \propto n^s$, where $s = 0{\cdot}33 \pm 0{\cdot}02$, that is $N_S A \propto n^{1/3}$, proportional to the average separation of impurity centres. As a further exercise we assumed that SC scattering was present in crystals 3LE132 and 7LE103, and found we could fit the experimental data taking the lower values for our deformation potentials, that is (E_1) 5 eV and (D_{XX}) 8×10^8 eV cm^{-1}. The values for $N_S A$ were $1{\cdot}6 \times 10^5$ cm^{-1} and $< 1{\cdot}0 \times 10^5$ cm^{-1}. We stress that the results for both crystals could be fitted without resorting to SC scattering, but the values for $N_S A$ lie well on the empirical curve shown in figure 13, to lower carrier concentrations and help to explain the slightly lower mobility values at 300 K in

these ⟨111⟩ samples than have been determined previously (Pitt and Lees 1970). Thus if we take the upper limits for D_{XX} of $1{\cdot}2 \times 10^9$ eV cm^{-1} and 7 eV (E_1) we obtain a mobility at 300 K which is much lower than is obtained experimentally on the purer material used by Pitt and Lees (1970). This strongly suggests that the lower paired values of D_{XX} and E_1, that is 8×10^8 eV cm^{-1} and 5 eV respectively, are more likely to be correct, and that the lower X_{1c} mobilities in these samples are a consequence of the space charge scattering which seems to be inherently present in crystals grown on a ⟨111⟩ face. The separate mobilities using these parameters were $\mu_{DP} = 2{\cdot}9 \times 10^3$ cm^2 V^{-1} s^{-1}, $\mu_{PO} = 1100$ cm^2 V^{-1} s^{-1}, $\mu_{IV} = 500$ cm^2 V^{-1} s^{-1}.

We have observed two activation energies for donor impurities to the ⟨100⟩ minima. These have been tentatively assigned in § 5.2 to Se or Sn levels after comparison with the S level data of Craford *et al* (1968). But in some of our samples, for example 244F, only the shallower level was observed rather than the deep level which should dominate all carrier results near 300 K. Thus the two levels were not consistently present. This is an argument against the two Se level hypothesis since we might expect them both to be present always. The whole problem of the existence of levels which lie degenerate with the lower lying conduction band minimum, yet whose wavefunctions are derived from higher lying minima, is exceedingly confusing. This is particularly the case for deep nonhydrogenic levels which have been observed in, for example, InAs (Pitt and Vyas 1973) and CdTe (Iseler *et al* 1972). These levels have been attributed to the higher states largely because the pressure coefficients of the impurity levels have corresponded with those for the minima. Callaway and Hughes (1967) have considered the effect of a vacancy in Si and find that the dominant contribution to the deep level impurity wavefunction comes from the valence band. It is conceivable that this level could lie higher in energy than the conduction band minimum. The valence band tends to decrease in energy at a rate comparable to that of the X_{1c} minima (ie ~ -1 to -2×10^{-6} eV bar^{-1}), and so some confusion could exist as to whether the level was associated with the valence band if the pressure coefficient of the level is of this order. Levels in InAs and CdTe have pressure coefficients near $+6 \times 10^{-6}$ eV bar^{-1} and these must be associated with the conduction band since it is only here that the large positive coefficients exist. Our levels in GaAs however, were assumed to have coefficients of -1×10^{-6} eV bar^{-1} and so we must be cautious about assigning the deep level to the X_{1c} minima. Measurements on Se doped $GaAs_{1-x}P_x$ alloys near the indirect–direct transition by Pitt and Stewart (1973) have revealed again the existence of two levels relative to the X_{1c} minima. By varying the stoichiometry and carrying out cathodoluminescence measurements to observe the emission of a peak at 1·2 eV, it was tentatively concluded that the deeper level was associated with a Ga vacancy complex. It would be interesting therefore to carry out a calculation along the lines of Callaway and Hughes (1967) to determine the properties of any level in GaAs due to this vacancy and to find where the dominant wavefunction contributions come from.

Acknowledgments

We wish to thank Professor P N Butcher and Drs W Fawcett, H D Rees, C Hilsum, K Fletcher and J Lees for helpful suggestions and Mr V Grant for technical assistance. The ⟨111⟩ epitaxial crystals were kindly grown for us by Dr P D Greene. The work was supported by a Ministry of Defence (Procurement Executive) contract. One of us (RAH) carried out some of the work in part fulfilment of a CAPS studentship with STL.

References

Adler P N 1969 *J. appl. Phys.* **40** 3554–5

Buchenauer C, Cerdeira F and Cardona M 1971 *Light Scattering in Solids* ed M Balkanski (Paris: Flammarion) pp 280–3

Callaway J and Hughes A J 1967 *Phys. Rev.* **156** 860–76

Conwell E M 1966 *Phys. Lett.* **21** 368–9

Conwell E M and Vassell M O 1968 *Phys. Rev.* **166** 797–821

Costato M and Reggiani L 1970 *Lett. Nuovo Cim.* **4** 848–57

Craford M G, Stillman G E, Rossi J A and Holonyak N 1968 *Phys. Rev.* **168** 857–82

Ehrenreich H 1959 *J. Phys. Chem. Solids* **8** 130–5

Epstein A S 1966 *J. Phys. Chem. Solids* **27** 1611–21

Fawcett W, Boardman A D and Swain S 1969 *J. Phys. Chem. Solids* **31** 1963–90

Fawcett W and Paige E G S 1971 *J. Phys.* C: *Solid St. Phys.* **4** 1801–21

Fletcher K and Butcher P N 1973 *J. Phys.* C: *Solid St. Phys.* to be published

Herbert D C, Fawcett W, Lettington A H and Jones D 1972 *Proc. 11th Int. Conf. Phys. Semiconductors, Warsaw* (in press)

Herring C 1955 *Bell System Tech. J.* **34** 237–90

Hilsum C 1965 *Prog. Semicond.* **9** 137

Iseler G W, Kafalas J A, Strauss A J, Macmillan H F and Bube R H 1972 *Solid St. Commun.* **10** 619–22

James L M and Moll J L 1969 *Phys. Rev.* **183** 740–53

Jorgensen M H, Gram N O and Meyer N I 1972 *Solid St. Commun.* **10** 337–40

Long D 1960 *Phys. Rev.* **120** 2024–32

McSkimin H F, Jayaraman A and Andreatch P Jr 1967 *J. appl. Phys.* **8** 2362–4

Montgomery H C 1968 *J. appl. Phys.* **39** 2002–5

Pitt G D 1968 *J. Phys.* E: *Sci. Instrum.* **1** 915–7

Pitt G D and Lees J 1970 *Phys. Rev.* B **2** 4144–60

Pitt G D and Stewart C E E 1973 to be published

Pitt G D and Vyas M K R 1973 *J. Phys.* C: *Solid St. Phys.* **6** 274–84

Rode D L 1970 *Phys. Rev.* B **2** 1012–24

—— 1972 *Phys. Stat. Solidi* B **53** 245–54

Streitwolf H W 1970 *Phys. Stat. Solidi* **37** K47

Toyama M, Naito M and Kasami A 1969 *Jap. J. appl. Phys.* **8** 358–65

Waugh J L T and Dolling G 1963 *Phys. Rev.* **132** 2410

Weisberg L R 1961 *J. appl. Phys.* **33** 1817–21

Wolfe C M, Stillman G E and Dimmock J O 1969 *J. appl. Phys.* **41** 504–7

Zawadzki W and Szymanska W 1972 *J. Phys. Chem. Solids* **32** 1151–74